First-principles investigations of the magnetic properties of graphite boron nitride sheet induced by Fe doping

2010 J. Phys.: Condens. Matter 22 205501

(http://iopscience.iop.org/0953-8984/22/20/205501)

J. Phys.: Condens. Matter **22** (2010) 205501 (5pp) doi:10.1088/0953-8984/22/20/205501

First-principles investigations of the magnetic properties of graphite boron nitride sheet induced by Fe doping

Xiaohui Deng[1], **Wenwei Wang**[1], **Dengyu Zhang**[1], **Wei Lu**[2] and **Bingbing Fan**[3,4]

[1] Department of Physics and Electronic Information Science, Hengyang Normal University, Hengyang 421008, People's Republic of China
[2] Department of Applied Physics, The Hong Kong Polytechnic University, Hung Hom, Kowloon, Hong Kong, People's Republic of China
[3] Center of Super-Diamond and Advanced Films (COSDAF) and Department of Physics and Materials Science, City University of Hong Kong, Hong Kong, People's Republic of China
[4] School of Materials Science and Engineering, Zhengzhou University, Henan, People's Republic of China

Received 2 January 2010, in final form 23 March 2010
Published 26 April 2010
Online at stacks.iop.org/JPhysCM/22/205501

Abstract
The first-principles spin polarization method is used to investigate the magnetic properties of graphite boron nitride (g-BN) sheet induced by Fe doping. We find that a nitrogen or boron atom substituted by Fe can induce a magnetic moment. From standard Mulliken population analysis, we also find that the magnetic moment is mainly dominated by Fe 3d states. Using Heisenberg exchange coupling theory, we study the exchange coupling mechanisms by constructing two-Fe centers in g-BN. The results show the presence of relatively strong exchange coupling for two-Fe substituted two-B atoms and the coupling is ferromagnetic. For the case of two-Fe substituted two-N atoms, the coupling is antiferromagnetic and the exchange coupling is very weak. The paper enriches recent molecular magnetic investigations.

(Some figures in this article are in colour only in the electronic version)

Recently there has been increasing interest in the field of light element nanostructures, such as graphite, fullerene, and carbon and boron nitrogen (BN) nanotubes [1–7]. In particular, the weak ferromagnetism in these compounds has attracted considerable attention due to their stimulation of molecular magnets, which could be applied in a high temperature environment. It is also found that spin polarization could be induced by vacancy, impurity, and substitution in these systems. Esquinazi *et al* [8] detected a ferromagnetic signal from an oriented graphite that behaved quite differently from known magnetic impurities, suggesting an intrinsic origin of magnetism in graphite. Ma *et al* [9] studied the magnetic properties of vacancies in graphite and carbon nanotubes. For graphite, the vacancy was spin polarized with a magnetic moment of 1.0 μ_B. The vacancy in carbon nanotubes could also induce magnetism, depending on their chirality and structure configuration with respect to the tube axis. Wu *et al* [10] found that carbon substitution in BN nanotubes can induce spontaneous magnetization.

However, until now the d0 ferromagnetism phenomena for graphite boron nitride sheet (g-BN) have not been reported experimentally. There are only a few theoretical studies concerning the electronic structure and magnetic properties of defects in the BN system [11, 12]. Si *et al* [13] found that intrinsic spontaneous magnetization could be induced by nitrogen or boron vacancies in g-BN. But the effects on magnetization of doping with the magnetic element Fe have not previously been investigated. In this paper, we carry out *ab initio* calculations to investigate electronic structure, magnetic properties, and magnetic coupling of these systems. Our calculations are performed using a linear combination of the atomic orbital (LCAO) method [14] within the framework of the density functional theory (DFT) implemented in the SIESTA [15, 16] code. For the exchange correlation functional

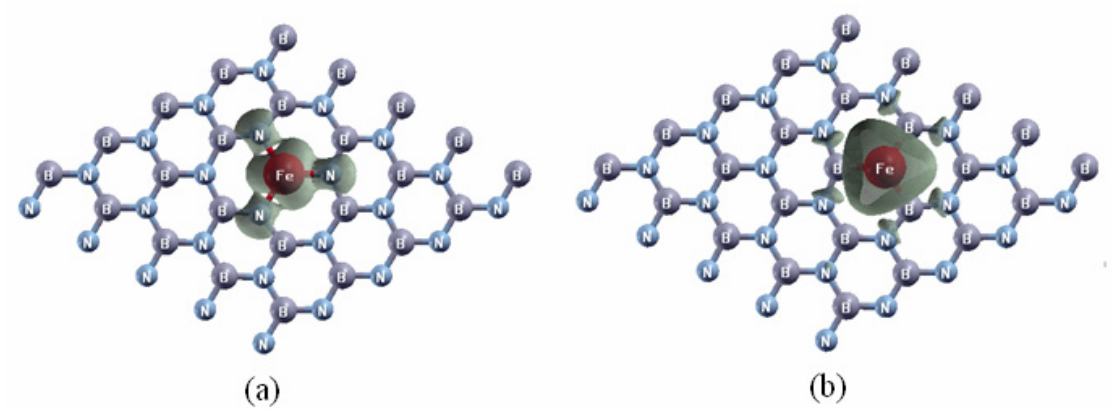

Figure 1. The structure and spin density distribution map of (a) the S^{B}_{Fe} case and (b) the S^{N}_{Fe} case. The isodensity surface values are 0.004 eV Å^{-3} in (a) and 0.0001 eV Å^{-3} in (b).

we choose the generalized gradient approximation (GGA) proposed by Perdew *et al* [17]. The interaction between ions and electrons is described by the pseudopotential generated by Troullier and Martins' scheme [18]. The double-ζ plus polarization atomic orbital basis set is employed in calculations. The charge density project on a real space grid and an equivalent plane wave cutoff energy of 200 Ryd is used. A $5 \times 5 \times 1$ Monkhorst–Pack grid [19] is set for Brillouin zone sampling. The conjugate gradient minimization scheme [20] is used to perform atom position relaxation and cell optimization. The XCRYSDEN program [21] is adopted to calculate the electronic spin density of state (SDOS).

We study first the system of a one-Fe and g-BN sheet. Two models, i.e. Fe substituted for a B or an N atom, named as S^{B}_{Fe} or S^{N}_{Fe}, are used. A 50-atom supercell is used to simulate a $5 \times 5 \times 1$ pristine g-BN sheet. By randomly substituting a B or an N atom with Fe, the impure systems S^{B}_{Fe} and S^{N}_{Fe} are constructed. Periodical boundary conditions are employed and adjacent layers are separated by a vacuum region of 20 Å. The supercells for pristine g-BN, the B substituted case S^{B}_{Fe}, and the N substituted case S^{N}_{Fe} are fully optimized without any constraints upon them. The final structures of S^{B}_{Fe} and S^{N}_{Fe} refer to figures 1(a) and (b). After relaxation, the Fe atom remains in the plane whether we initially place an Fe atom in the g-BN plane or not, which support the idea that the plane structures are the lowest energy structures. In the case of S^{B}_{Fe}, lattice length a (or b) increases from 12.54 to 12.66 Å. With Fe substituted B, three adjacent N atoms expand outward. The final distances between Fe and N are 1.79 Å. Atom configurations far from Fe remain almost unchanged compared with pristine g-BN. The B–N distance is 1.46 Å and that in pristine g-BN is 1.45 Å. In the case of S^{N}_{Fe}, with Fe substituted N, the local symmetry of pristine g-BN is broken. The distances between Fe and three adjacent B atoms are 1.74 Å, 1.76 Å, and 1.76 Å, respectively. The Fe–N distances in the case of S^{B}_{Fe} are larger than the Fe–B distances in the case of S^{N}_{Fe}. We point out that our B–N distance in pristine g-BN is 1.45 Å according to that reported by Si *et al* [13]. In order to quantify the ability of forming of these substituted systems, we calculate the formation energy E_{form} with the following expression

$$E_{form}[S^{i}_{Fe}] = E_{tot}[S^{i}_{Fe}] - E_{tot}[\text{g-BN, pristine}] + \mu_i - \mu_{Fe}, \quad (1)$$

where $E_{tot}[S^{i}_{Fe}]$ is the total energy of a supercell of S^{B}_{Fe} or S^{N}_{Fe}, E_{tot}[g-BN, pristine] is the total energy of the corresponding pristine g-BN supercell, μ_i is the chemical potential of atom B or N, and μ_{Fe} is the chemical potential of atom Fe. We take nitrogen gas for μ_i of N and α-rhombohedral B_{12} for B. μ_{Fe} is taken from body-centered cubic (BCC) Fe. The obtained E_{form} of S^{B}_{Fe} and S^{N}_{Fe} are 13.0 and 11.4 eV, indicating that the S^{N}_{Fe} case is more likely to form than the S^{B}_{Fe} case. Si *et al* [13] reported the N or B vacancy formation energy in g-BN. We also calculate the vacancy formation energy to be 10.7 eV and 8.5 eV for V_B and V_N, respectively, which is consistent with results by Si *et al* [13] (9.99 and 8.33 eV). One can find that the formation of S^{B}_{Fe} and S^{N}_{Fe} must firstly break the B–N bond and provide 10.7 eV and 8.5 eV, respectively. Fe located in the B or N position only needs 2.3 and 2.9 eV for two defects. The formation energies are relatively large, which is attributed to their strong B–N bond energy in such sp^2-bonded systems.

In order to investigate magnetic properties induced by Fe substituted B or N. the electronic densities of states (DOSs) are calculated. The obtained DOSs near the Fermi energy (E_f) are shown in figures 2(b) and (c). For compassion, that of pristine g-BN is shown in figure 2(a). It can be found that the ground state of pristine g-BN is non-spin-polarized and the magnetic moment is zero. But because of doping of Fe, the pristine g-BN are spin polarized. In the case of S^{B}_{Fe}, near the Fermi energy, the majority DOS is different from the minority DOS. A significant peak occupied by majority spin electrons and minority spin peaks weakens. The half-metallic behavior is also found. The majority spin component possesses a band gap while the minority spin component is metallic. Such half-metallic behavior also was found in other doped systems [13, 22, 23]. Therefore, the S^{B}_{Fe} case is expected to have a big magnetic moment. But in the S^{N}_{Fe} case, spin polarization behavior is not obvious. The minority DOSs only shift forward compared with the majority DOSs near E_f.

In order to understand the influence of the Fe substitution on magnetism, we analyze the interaction between the orbital of the Fe and the g-BN from the calculated electronic spin DOS. In figures 2(b) and (c) we present the contribution of the 3d partial DOS (PDOS) of Fe atoms to compare with the total

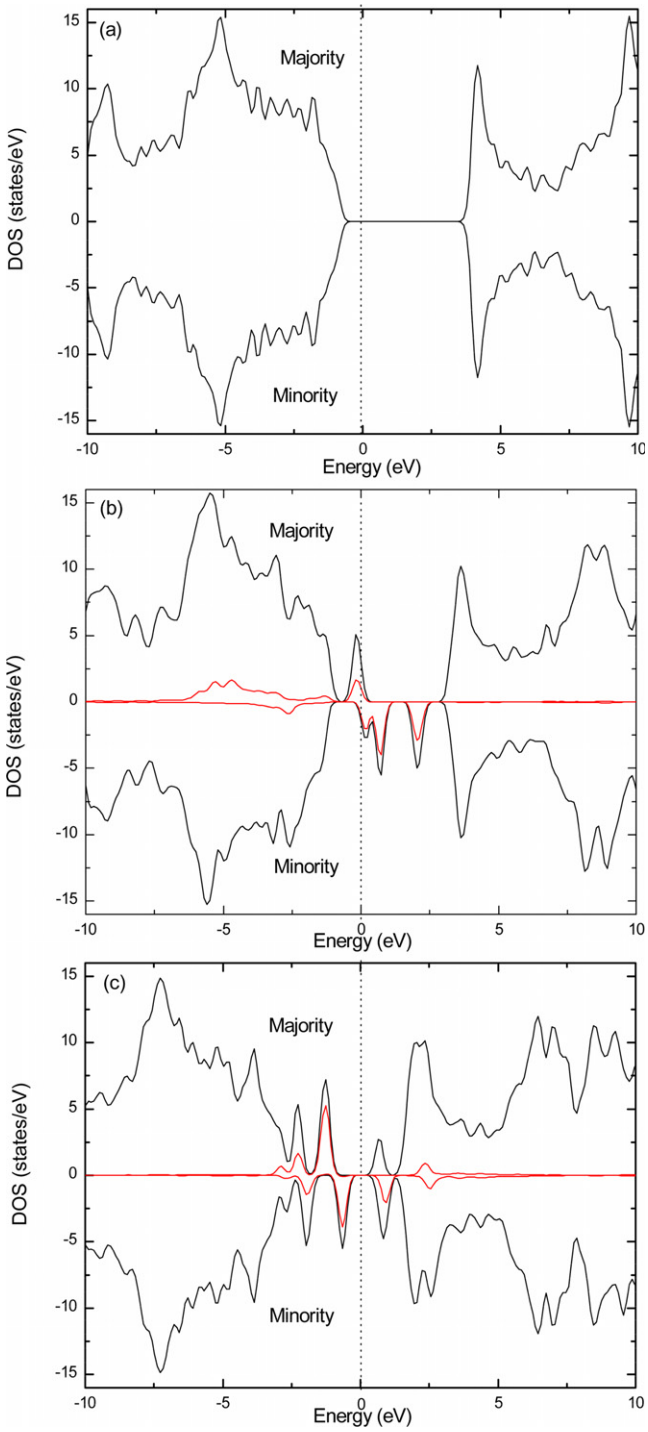

Figure 2. The calculated total majority and minority DOS and PDOS of the Fe 3d orbital (black and red lines, respectively) of (a) pristine g-BN, (b) the $S_{\mathrm{Fe}}^{\mathrm{B}}$ case, and (c) the $S_{\mathrm{Fe}}^{\mathrm{N}}$ case. The Fermi energy is set to zero by a dotted line.

DOS. The pictures show that the energy of Fe 3d is mainly concentrated near E_{f}, and the total DOS near E_{f} are mainly dominated by the Fe 3d states. The minority spin of Fe 3d states moves right relative to that of the majority, indicating the spin splitting near the Fermi energy level in both cases. From figure 2, we also find that the proportion of Fe 3d states to total DOS in $S_{\mathrm{Fe}}^{\mathrm{B}}$ is relatively lower; however, that in $S_{\mathrm{Fe}}^{\mathrm{N}}$ is relatively higher. So we conclude that the contribution of other atoms or orbitals to magnetism in $S_{\mathrm{Fe}}^{\mathrm{B}}$ is bigger than that in $S_{\mathrm{Fe}}^{\mathrm{N}}$. The quantity analysis will be carried out in the following part to make this point clear.

Table 1. Magnetic moments M_{Fe} (in μ_{B}) and occupied electron numbers of the Fe atom in substituted g-BN and in bulk Fe from Mulliken population analysis. P_{p} indicates polarized orbital. ↑ and ↓ indicate spin up and spin down.

	M_{Fe}	Total↑	Total↓	3d↑	3d↓	4s↑	4s↓	$4p_p$↑	$4p_p$↓
$S_{\mathrm{Fe}}^{\mathrm{B}}$	3.953	5.679	1.726	4.793	1.173	0.436	0.259	0.450	0.294
$S_{\mathrm{Fe}}^{\mathrm{N}}$	1.324	4.604	3.280	3.804	2.741	0.726	0.474	0.074	0.065

The total magnetic moment of $S_{\mathrm{Fe}}^{\mathrm{B}}$ is 5.0 μ_{B} and the isosurface of spin density at 0.004 eV Å^{-3} is shown in figure 1(a), from which one can find that the magnetic moment mainly comes from Fe and three adjacent N atoms. Fe donates 3.953 μ_{B} and every N 0.219 μ_{B}. For the main donor Fe atom, from standard Mulliken population analysis, we note that spin polarization mainly comes from its 3d orbital with a value of 3.529 μ_{B}. The s orbital of the Fe atom donates 0.207 μ_{B}. For the case of $S_{\mathrm{Fe}}^{\mathrm{N}}$, the total magnetic moment is 1.0 μ_{B}. In figure 1(b), we plot the isosurface of spin density at 0.0001 eV Å^{-3}. From figure 1(b), one notices that the spin density also comes from the Fe atom. But for three adjacent B atoms, their electronics is almost non-spin-polarized. The rest of the magnetic moment comes from six adjacent N atoms polarized directly by Fe. We compile the occupied electronic number and magnetic moments of Fe in table 1. For the $S_{\mathrm{Fe}}^{\mathrm{B}}$ case, the magnetic moment of the Fe atom is 3.953 μ_{B}, which is larger than that in bulk Fe (2.352 μ_{B}). This is because some spin down electrons become spin up in $S_{\mathrm{Fe}}^{\mathrm{B}}$ compared with in bulk Fe. In the $S_{\mathrm{Fe}}^{\mathrm{N}}$ case, the magnetic moment of the Fe atom is 1.324 μ_{B}. The 3d electron of Fe denotes 3.620 μ_{B} and 1.063 μ_{B} in $S_{\mathrm{Fe}}^{\mathrm{B}}$ and $S_{\mathrm{Fe}}^{\mathrm{N}}$, respectively. The ratios to total magnetic moment are ∼92% and 80%, supporting the fact that the magnetic moments mainly come from 3d states of the Fe atom.

We must point out that Mulliken population analysis is chosen as the method of assigning electrons to atoms or orbitals in this paper. Mulliken analysis provides a means of estimating partial atomic charges from our DFT calculations and it severely depends on the selection of basis sets. But we believe our results are reliable because of the accord of DOS of bulk Fe in this paper with well-known experimental results.

The mechanisms for a long range ferromagnetic order in this substituted system are finally discussed. A larger supercell, i.e. a 10 × 5 × 1 supercell including 100 atoms, is constructed with two-Fe atoms substituted by two-B or N atoms. The Fe–Fe interval has two-B or N atoms (figures 3 and 4). After relaxation, two-Fe atoms displace significantly out of plane and they arrange themselves automatically on both sides of the plane. The case of two Fe displacing the same direction has a slightly higher energy (∼1.0 eV). To study the exchange coupling between two-Fe centers, the Heisenberg Hamiltonian $\hat{H} = -J\hat{S}_1\hat{S}_2$ is employed. The exchange coupling constant is considered and this method can be found elsewhere [24–27]. After careful exploration

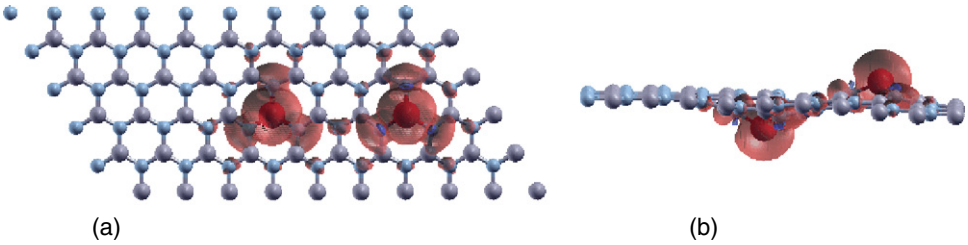

Figure 3. Spin density distribution of the ferromagnetic (FM) state for two-Fe substituted two-B atoms. (a) top view and (b) side view. The isodensity surface value is 0.0007 eV Å^{-3}. The red surface represents the spin up.

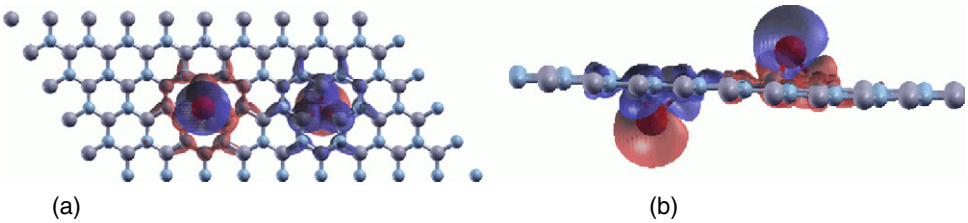

Figure 4. Spin density distribution of antiferromagnetic (AFM) for 2-Fe substituted two-N atoms. (a) is top view and (b) side view. The isodensity surface value is 0.0007 eV Å^{-3}. The red and blue surface represents the spin up and down, respectively.

of equilibrium structures, we calculate the total energies of both ferromagnetic and antiferromagnetic states. In the two-Fe substituted two-B case, the ferromagnetic state is favored over the antiferromagnetic one by a lower energy. The total magnetic moment is 10.0 μ_B and the antiferromagnetic one is zero. The spin density distribution for the ferromagnetic state is shown in figure 3. We note that the coupling of the two-Fe center is realized by the polarization of adjacent N atoms. The contribution from B atoms is smaller. The calculated exchange coupling constant J is 70.0 cm^{-1}, indicating a relatively strong coupling. In the two-Fe substituted two-N case, the ground state is antiferromagnetic with a zero magnetic moment. The spin of two Fe is completely anti-parallel. From the spin density map (figure 4), we find that the exchange path is the B–N–B–N–B chain. The communication between two-Fe centers is realized through this bridge. But the exchange coupling is very weak with an obtained J value of -2.6 cm^{-1}. Based on the discussion above, we conclude that Fe substitution in the g-BN sheet can realize magnetic communication by controlling B vacancies. To discuss the formation ability, we also consider two extra cases, i.e. a two-Fe substituted adjacent B and N pair ($S^{\mathrm{BN}}_{2\mathrm{Fe}}$) and a third-neighboring B and N pair ($S^{\mathrm{BN}'}_{2\mathrm{Fe}}$, the Fe–Fe interval has two-B or N atoms too), for charge compensation reasons. The calculated formation energies of $S^{2\mathrm{B}}_{2\mathrm{Fe}}$, $S^{2\mathrm{N}}_{2\mathrm{Fe}}$, $S^{\mathrm{BN}}_{2\mathrm{Fe}}$, $S^{\mathrm{BN}'}_{2\mathrm{Fe}}$ are 16.7, 19.07, and 17.5, 18.2 eV, indicating that the $S^{2\mathrm{B}}_{2\mathrm{Fe}}$ case is more likely to form than the rest. The cross-doped pair case possesses the middle formation ability. The ground states of the two cross-doped cases are ferromagnetic with a magnetic moment of 6.0 μ_B and 4.0 μ_B, respectively.

B vacancies are important to realize the magnetic communication because of strong coupling in the $S^{2\mathrm{B}}_{2\mathrm{Fe}}$ system. But the B–N bond is firstly broken. The bond energy of such sp^2 is commonly large. Recently, oxidation has become an interesting way to realize the cracking of sp^2- or sp^3-bonded systems. But, once defects occur, Fe doping becomes easier. From the analysis about formation energy, for example for $S^{\mathrm{B}}_{\mathrm{Fe}}$ and $S^{\mathrm{N}}_{\mathrm{Fe}}$, one can find that their formation must provide 13.0 and 11.4 eV, respectively. The corresponding defects need 10.7 and 8.5 eV. In other words, Fe locating at the B or N position only needs 2.3 and 2.9 eV.

In summary, we have performed first-principles spin polarization calculations to investigate the magnetic properties of graphite boron nitride (g-BN) sheet induced by doping with Fe. The obtained formation energy indicates that the $S^{\mathrm{B}}_{\mathrm{Fe}}$ case is more likely to form than the $S^{\mathrm{N}}_{\mathrm{Fe}}$ case. Our system considered here possesses a magnetic moment (1.0 μ_B and 5.0 μ_B for $S^{\mathrm{N}}_{\mathrm{Fe}}$ and $S^{\mathrm{B}}_{\mathrm{Fe}}$, respectively). Doping of Fe into vacancies of B enlarges the total magnetic moment, which can be attributed to the fact that Fe polarizes the adjacent B atoms. By electronic structure calculations, a half-metallic behavior is found in the $S^{\mathrm{B}}_{\mathrm{Fe}}$ case. The magnetic moment is mainly dominated by Fe 3d states from standard Mulliken population analysis. Using Heisenberg exchange coupling theory, we point out the exchange coupling mechanisms by constructing two-Fe centers in g-BN. The obtained J values predict strong ferromagnetic coupling in the two-Fe substituted two-B atoms case and very weak antiferromagnetic coupling in the two-Fe substituted two-N atoms case. The present work enriches recent molecular magnet investigations and indicates a way to increase magnetism by doping with a magnetic element.

Acknowledgment

The authors would like to acknowledge financial support from the Scientific Research Fund of the Hunan Provincial Education Department under grant No. 09A013.

References

[1] Wong S S, Joselevich E, Woolley A T, Cheung C L and Lieber C M 1998 *Nature* **394** 52

[2] Ajayan P M 1999 *Chem. Rev.* **99** 1787
[3] Banhart F 1999 *Rep. Prog. Phys.* **62** 1181
[4] Bochrath M, Liang W L, Bozovic D, Hafner J H, Lieber C M, Tinkham M and Park H 2001 *Science* **291** 283
[5] Ouyang M, Huang J L, Cheung C L and Lieber C M 2001 *Science* **291** 97
[6] Woodside M T and Mceuen P L 2002 *Science* **296** 1098
[7] Samsonidze G G, Samsonidze G G and Yakobson B I 2002 *Phys. Rev. Lett.* **88** 065501
[8] Esquinazi P, Setzer A, Hohne R, Semmelhack C, Kopelevich Y, Spemann D, Butz T, Kohlstrunk B and Losche M 2002 *Phys. Rev.* B **66** 024429
[9] Ma Y, Lehtinen P O, Foster A S and Nieminen R M 2004 *New J. Phys.* **6** 68
[10] Wu R Q, Liu L, Peng G W and Feng Y P 2005 *Appl. Phys. Lett.* **86** 122510
[11] Orellana W and Chacham H 2001 *Phys. Rev.* B **63** 125205
[12] Schmidt T M, Baierle R J, Piquini P and Fazzio A 2003 *Phys. Rev.* B **67** 113407
[13] Si M S and Xue D S 2007 *Phys. Rev.* B **75** 193409
[14] Artacho E, Sánchez-Portal D, Ordejón P, García A and Soler J M 1999 *Phys. Status Solidi* b **215** 809
[15] Soler J M, Artacho E, Gale J D, García A, Junquera J, Ordejón P and Sánchez-Portal D 2002 *J. Phys.: Condens. Matter* **14** 2745
[16] Ordejón P, Artacho E and Soler J M 1996 *Phys. Rev.* B **53** R10441
[17] Perdew J P, Burke K and Ernzerhof M 1996 *Phys. Rev. Lett.* **77** 3865
[18] Troullier N and Martins J L 1991 *Phys. Rev.* B **43** 1993
[19] Monkhorst J and Pack J D 1976 *Phys. Rev.* B **13** 5188
[20] Bylander D M, Kleinman L and Lee S 1990 *Phys. Rev.* B **42** 1394
[21] Kohalj A 2003 *Comput. Mater. Sci.* **28** 155
[22] Ye L H, Freeman A J and Delley B 2006 *Phys. Rev.* B **73** 033203
[23] Si M S and Xue D S 2006 *Europhys. Lett.* **76** 664
[24] Si M S and Xue D S 2008 *Appl. Phys. Lett.* **92** 081907
[25] Ruiz E, Nunzi F and Alvarez S 2006 *Nano Lett.* **6** 380
[26] Ruiz E, Rodríguez-Fortea A, Cano J, Alvarez S and Alemany P 2003 *J. Comput. Chem.* **24** 982
[27] Ruiz E, Cano J, Alvarez S and Alemany P 1999 *J. Comput. Chem.* **20** 1391